

# Luminescence properties of submicron features fabricated by using magnetron reactive ion etching with different sample biases

M. Freiler

*Columbia Radiation Laboratory, Columbia University, New York, New York 10027*

G. F. McLane

*U.S. Army Research Laboratory, Fort Monmouth, New Jersey 07703*

S. Kim, M. Levy, R. Scarmozzino, I. P. Herman, and R. M. Osgood, Jr.

*Columbia Radiation Laboratory, Columbia University, New York, New York 10027*

(Received 8 August 1995; accepted for publication 10 October 1995)

Deep-etch-defined GaAs/Al<sub>0.3</sub>Ga<sub>0.7</sub>As square features of multiquantum well material, with dimensions as small as 160 nm, have been fabricated using magnetron reactive ion etching (MIE). Luminescence spectroscopy shows confinement of charge carriers to the features' center. The effects of rf power and etching time on the luminescence efficiency of these features and its concomitant etch-induced damage are examined. © 1995 American Institute of Physics.

There has been much recent interest in the use of dry etching in the fabrication of ~100 nm scale features in semiconductor electronic and photonic devices.<sup>1,2</sup> Often, though, the application of dry etching leads to bulk or near-surface (note we are distinguishing between damage caused by changes in the bulk or near-surface material and the deleterious effects due to surface impurities) material damage due to energetic particle bombardment of the sample sidewall; this damage limits the performance of devices based on these features.<sup>2,3</sup> One approach to the reduction of this damage is the use of high-density plasma etching, where the reactant flux is high, and the relative importance of energetic-ion-bombardment is diminished. Magnetron-enhanced reactive ion etching (MIE) is a particularly promising approach to such high-density, low-damage etching,<sup>4</sup> in fact, MIE of GaAs substrates results in low damage and high etch rates relative to conventional reactive ion etching (RIE).<sup>5</sup>

In this letter, the use of MIE for the fabrication of ~160–1500 nm semiconductor boxes in GaAs/Al<sub>0.3</sub>Ga<sub>0.7</sub>As is described. The luminescence properties of these features are measured as a function of the plasma-etching parameters. It is found that, for the plasma conditions examined here, decreasing the ion energy by varying, for example, the sample bias results in an *increase* of the near-surface damage to the etched sidewalls. This procedure allows “tuning” of the degree of sample damage, allowing the reduction of near-surface, bulk damage to the sample sidewall. Also presented is evidence for lateral confinement of the photoexcited charge carriers due to electrostatic bandbending. These results show that under proper operation, MIE may be a promising technique for pattern transfer in the fabrication of nanostructures.

To evaluate the use of MIE for deep-submicron feature fabrication, a test pattern was etched by MIE into a multiple-quantum-well substrate. The substrate consisted of 3, 50 Å, GaAs quantum wells (QWs), separated by 250 Å Al<sub>0.3</sub>Ga<sub>0.7</sub>As barriers, and a 50 Å GaAs cap, grown by MOCVD on a SI GaAs (100) substrate. The three QWs were sufficiently close to the surface that all absorbed significant excitation light; thus the use of three QWs served to enhance

the PL signal which was degraded by the small geometric fill factor and a metal-capping layer (see below) of the sample array. All epitaxial material was unintentionally doped. The pattern consisted of 240 μm square arrays containing uniform-size squares ranging from 250 to 2000 nm in linear dimension. The pattern also had a large (250 μm × 1000 μm), mask-covered area, which was used to determine the luminescence of unetched material. The mask was fabricated at the Cornell Nanofabrication Facility using electron-beam lithography of a 250 Å Au/50 Å Cr thin film. Etch experiments were performed in an MRC 710 magnetron reactive-ion etch system. The boxes were fabricated by using MIE over a 1000 cm<sup>2</sup> area in BCl<sub>3</sub> to etch the patterned samples. The MIE chamber pressure was 2 mTorr and the BCl<sub>3</sub> flow rate was 2 sccm. Samples were etched with various combinations of rf power (correlating with sample bias) and etch time to examine the effects of the etching process on the properties of these boxes. Note the exposure of the feature sidewalls to the plasma increased with the etch depth.

Photoluminescence (PL) measurements were conducted to determine the quality of the etched structures. The samples were removed from the MIE chamber and PL was measured without any further surface treatment. Only the PL signal from the quantum-well region was measured. Both the 20 mW, 488 nm excitation beam from an Ar<sup>+</sup> laser and the luminescence collection were normal to the sample surface. The excitation beam was focused to a 20 μm spot size, which presented useful spatial resolution but was large enough to prevent significant laser-induced sample heating (i.e., <2 K). Note also that the PL signal responded linearly to changes in the laser power and that no permanent laser-induced PL changes in the samples' photoresponse were seen. The excitation laser and luminescence signal intensity were attenuated by ~50× by the metal etch mask, which was left on the sample so as to prevent any possible damage or alteration to the sample which might be incurred during chemical removal of the metal.

For each array of constant-sized features, both the luminescence spectrum of the etched features and the peak luminescence signal were recorded. In all the cases, the etching

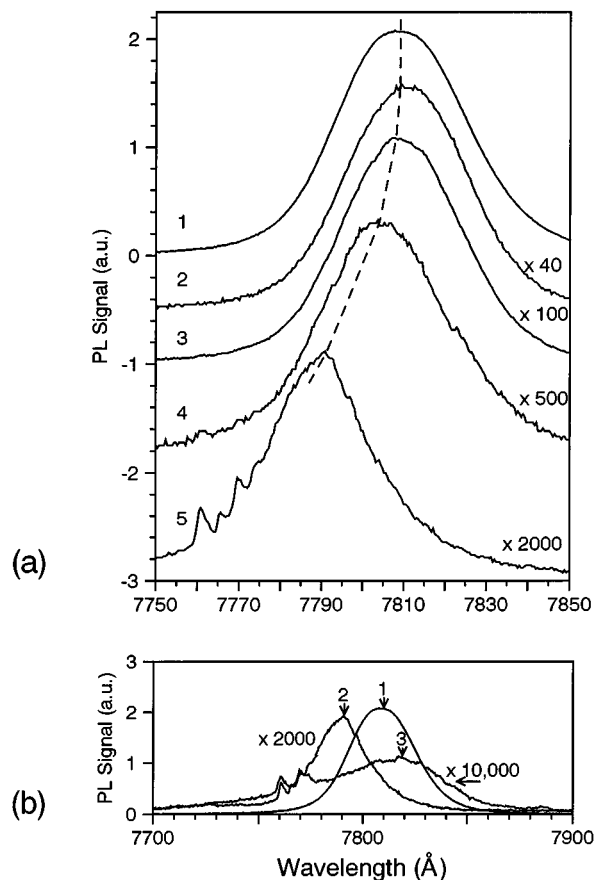


FIG. 1. (a) Quantum-well luminescence spectra for (1) unetched, (2) 1300 nm, (3) 680 nm, (4) 330 nm, and (5) 160 nm features on a 75 V bias sample etched to 290 nm. (b) Quantum-well luminescence spectra for (1) an unetched sample, (2) 190 nm features etched to 290 nm using 75 V bias, and (3) 170 nm features etched to 310 nm using 30 V bias.

was sufficiently deep to remove all quantum-well materials. Detailed examination of the PL signal from the unmasked, etched areas showed no evidence of quantum-well luminescence in these regions. Many regions of constant feature size were investigated for any nonuniformities in the magnitude of the luminescence signal; these were found to be  $<10\%$ , slightly more than the 7% variation expected on the basis of the statistical variation of the number of quantum boxes within the excitation laser spot. The unetched quantum-well material was checked for uniformity by measuring the variation of the luminescence peak energy in unetched regions across the sample. The sample was found to be highly uniform, with a variation of  $\pm 0.3$  meV ( $\pm 2$  Å) in the position of peak luminescence photon energy. Variations in this PL peak energy of etched features were studied for 1000 and 2000 nm boxes of constant etch depth. These were found to be the same as the unetched samples. Smaller features exhibited blue-shifted spectra depending on the feature size. All spectra were of the same shape and had the same full width at half-maximum as those for the unetched regions, except for the smallest features of the 30 V bias samples, as discussed below. Typical spectra are shown in Fig. 1. The normalized luminescence efficiency was found by dividing the peak luminescence signal by the geometric fill factor and the peak-luminescence signal of a large masked area of unetched ma-

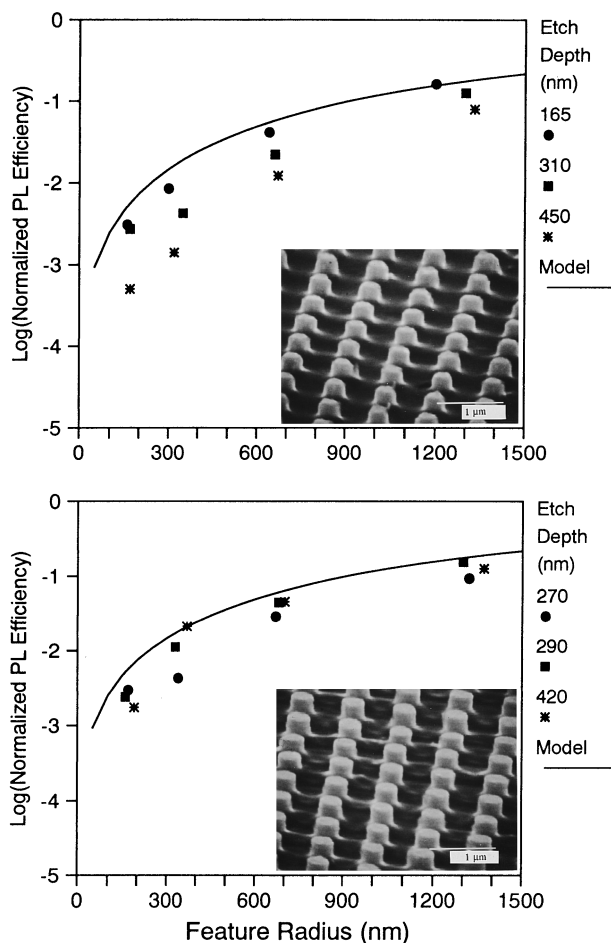


FIG. 2. Luminescence efficiency vs feature radius of disks etched to various depths using (a)  $0.2$  W/cm<sup>2</sup> rf-power density, giving 30 V dc bias and (b) using  $0.4$  W/cm<sup>2</sup> rf-power density, giving 75 V dc bias. In both (a) and (b) the solid lines are from a model described in Ref. 6 for the luminescence of features etched using damage-free etching. Inset: (a) array of 170 nm features from the 310 nm etched sample. Inset: (b) array of 190 nm features from the 290 nm etch depth sample.

terial. These results were corrected, where needed, for variations in the luminescence lineshape.

Figure 2(a) shows the logarithm of the luminescence efficiency as a function of the feature effective radius for the  $0.2$  W/cm<sup>2</sup>, 30 V biased samples, etched to different etch depths. For the smaller feature sizes, the luminescence efficiency decreased as the exposure time increases. These results indicate MIE at this sample bias induces bulk damage to the etched-feature sidewall, and that this damage increases as the sidewall is exposed to the plasma, a process most readily detected in small-dimension boxes. For comparison, the solid line in this figure represents the expected luminescence efficiency for undamaged features, obtained from a model calculation which includes only drift diffusion of minority charge carriers and nonradiative recombination at the feature surface.<sup>2</sup> This model assumes a  $1$  μm carrier diffusion length and a surface nonradiative recombination velocity of  $10^6$  cm/s; values which are consistent with earlier studies of the luminescence of boxes fabricated with wet etching and photon-driven cryoetching, and subsequently exposed to

atmospheric oxygen, both of which induce minimal bulk damage.<sup>6</sup> The model can also determine the effective thickness of any possible near-surface damage layer (by linearly shifting the measured feature radius). For example, for the sample etched to 165 nm, this damage layer must be <100 nm. For the 310 nm sample, the damage layer is 50–150 nm, and for the 450 nm sample, 150–250 nm. The results in Fig. 2(a) should be compared with the logarithm of the luminescence efficiency as a function of feature radius for samples etched with a 75 V bias (0.4 W/cm<sup>2</sup> rf power density). In this case, the luminescence efficiency is independent of the etch depth and is very close to the model curve. The results in Fig. 2(b) suggest that etching with the higher voltage does not significantly damage the feature sidewalls, since the model curve coincides with PL data obtained from features fabricated by wet etching.<sup>3</sup> Shifting the model curve along the positive  $x$  axis indicates that any damage layer, if present, must be <100 nm. Comparison with at least one example of data on reactive-ion etching<sup>2</sup> shows that MIE generates significantly less near-surface, bulk damage for comparable etch depths. Note that, in contrast to Ref. 2, we did not find any evidence of an increase in the size of the damage layer with etch depth, a further indication that at the higher bias voltage, the MIE generates little bulk damage.

The increase in damage as the sample bias is decreased is most likely due to an increase in the ion flux incident on the sidewalls. Possible reasons for this increase are an increase in beam divergence with lower ion energy,<sup>7</sup> or more deflection of the lower-energy ions by the local electric field<sup>8</sup> or the sidewall image-charge potential.<sup>9</sup> These findings appear to be opposite to earlier measurements, which show that sidewall near-surface damage increases with sample bias.<sup>10</sup> However, these earlier experiments were performed using much higher ion energies. In addition, the etched feature size and shape of our samples [inset, Figs. 2(a) and 2(b)] suggest that there is more sidewall ion bombardment for the 30 V sample than for the 75 V sample. The features on the 75 V sample had a somewhat larger average radius (190 nm) than that of the features on the 30 V sample (170 nm), suggesting that etching-induced erosion of the sample sidewalls is more significant in the latter case.

A comparison of the luminescence spectra of samples etched at 75 and 30 V bias also gives evidence of near-surface damage induced to the 30 V bias sample. Figure 1(b) shows the luminescence spectra of samples etched to 270 nm at 75 V and 290 nm at 30 V. The luminescence spectrum of the 75 V sample has the same shape and width as an unetched sample. The spectrum of the 30 V bias sample, however, is bimodal. We speculate that the shorter-wavelength peak originates from lattice disorder, which causes a relaxation of the  $k$ -selection rules for radiative quantum-well recombination, as seen by Kash *et al.*<sup>3</sup>

Changes in the photoluminescence spectrum as the feature size is varied show lateral confinement in these etched features. Figure 1 shows that for the sample etched with the 75 V bias to 290 nm depth, there is a small but clear blue shift in the luminescence peak energy that increases as the feature radius decreases; this shift was seen repeatedly for a

variety of samples with these sizes and etching conditions. For the 160 nm effective-radius feature on this sample, the blue shift is 3.7 meV. The extent of this shift is much larger than any expected blue shift due to simple hardwall, lateral, quantum confinement in features with these geometric dimensions. However, such a relatively large shift can be explained by additional spatial confinement of the photoexcited charge carriers at the feature center provided by near-surface electrostatic band bending at the feature sidewalls.

Specifically, because of upward band bending at the surface of unclad GaAs, a disc with a sufficiently small radius will be depleted of charge carriers, leaving a positive charge of ionized donors at the disk's interior. This interior positive charge will form a parabolic electrostatic potential well that confines the electrons to the disk center. The radius of a fully depleted quantum disk with a donor density  $N_D$  can be calculated using Gauss' Law. Assuming a typical value of 0.5 V (Ref. 11) for a pinned GaAs surface and  $N_D \sim 10^{16}/\text{cm}^3$  for undoped MOCVD material gives a value of  $\sim 350$  nm for the maximum radius of a fully depleted disk. In that case the zero-point energy in the conduction band is given by

$$E_e = h \sqrt{\frac{2N_D q}{\epsilon m}}$$

Since the hole mass is much larger than the conduction band mass,  $E_h \ll E_e$  and  $E_e$  should be equal to the spectral shift seen in our experiment. In fact, assuming  $N_D \sim 10^{16}/\text{cm}^3$  we estimate  $E_e \sim 3.0$  meV, in good agreement with our measurements. For the 330 nm features, the carriers are confined in a smaller disk of 45 nm by the depletion regions. Use of an equivalent hard-walled potential disk would give a shift of 1.4 meV, a value which compares favorably with the 1.2 meV blue shift actually measured.

The authors would like to thank Juni Fujita for his aid in the modeling of the data. The samples were patterned by Rick Bojko at Cornell University's National Nanofabrication Facility. This work has been generously funded by AFOSR/ARPA Contract No. F49620-92-J-0414 and JSEP Contract No. DAAH04-94-G-0057.

- <sup>1</sup>M. A. Reed, R. T. Bate, K. Bradshaw, W. M. Duncan, W. R. Frensley, J. W. Lee, and H. D. Shih, *J. Vac. Sci. Technol. B* **4**, 358 (1986).
- <sup>2</sup>E. M. Clausen, Jr., H. G. Craighead, J. M. Worlock, J. P. Harbison, L. M. Schiavone, L. Florenz, and B. Van der Gaag, *Appl. Phys. Lett.* **55**, 1427 (1989).
- <sup>3</sup>K. Kash, P. Grabbe, R. E. Nahory, A. Scherer, A. Weaver, and C. Caneau, *Appl. Phys. Lett.* **53**, 2214 (1988).
- <sup>4</sup>G. F. McLane, M. W. Cole, D. W. Eckart, P. Cooke, R. Moekirk, and M. Meyyappan, *J. Vac. Sci. Technol. B* **11**, 1753 (1993). Leareau, M. Namaroff, and J. Sasserath, *J. Vac. Sci. Technol. B* **11**, 333 (1993).
- <sup>5</sup>G. F. McLane, M. Mayyappan, M. W. Cole, and C. Wrenn, *J. Appl. Phys.* **69**, 695 (1991).
- <sup>6</sup>M. B. Freiler, S. Kim, M. Levy, M. C. Shih, R. Scarmozzino, I. P. Herman, and R. M. Osgood, Jr. (unpublished).
- <sup>7</sup>H. Gokan, M. Itoh, and S. Esho, *J. Vac. Sci. Technol. B* **2**, 34 (1984).
- <sup>8</sup>D. J. Economou and R. C. Alkire, *J. Electrochem. Soc.* **135**, 941 (1988).
- <sup>9</sup>R. J. Davis, *Appl. Phys. Lett.* **59**, 1717 (1991).
- <sup>10</sup>K. K. Ko, S. W. Pang, T. Brock, M. W. Cole, and L. M. Casa, *J. Vac. Sci. Technol. B* **12**, 3382 (1994).
- <sup>11</sup>W. E. Spicer, C. W. Chye, C. M. Garner, I. Lindau, and M. Pianetta, *Surf. Sci.* **86**, 363 (1979).